Adsorption (2012) 18:349–357
DOI 10.1007/s10450-012-9412-4

Effects of pore structure and surface chemical characteristics on the adsorption of organic vapors on titanate nanotubes

Chung-Kung Lee · Sheng-Kuo Fen · Huan-Ping Chao · Shin-Shou Liu · Fu-Chuang Huang

Received: 26 February 2012 / Accepted: 23 August 2012 / Published online: 5 September 2012

Abstract Effects of pore structure and surface chemical characteristics of titanate nanotubes (TNTs) on their adsorptive removal of organic vapors were investigated. TNTs were prepared via a hydrothermal treatment of TiO_2 powders in a 10 M NaOH solution at 150 °C for 24 h, and subsequently washed with HCl aqueous solution of different concentrations. Effects of acid washing process (or the sodium content) on the microstructures and surface chemical characteristics of TNTs were characterized with nitrogen adsorption-desorption isotherms, FTIR, and water vapor adsorption isotherms. For the adsorption experiments, gravimetric techniques were employed to determine the adsorption capacities of TNTs for four organic vapors with similar heats of vaporization (i.e., comparable heats of adsorption) but varying dipole moments and structures, including *n*-hexane, cyclohexane, toluene, and methyl ethyl ketone (MEK), at isothermal conditions of 20 and 25 °C. The experimental data were correlated by well-known vapor phase models including BET and GAB models. Isosteric heats of adsorption were calculated and heat curves were established. Equilibrium isotherms of organic vapors on TNTs were type II, characterizing vapor condensation to form multilayers. The specific surface area (and pore volume) and hydrophilicity of TNTs were the dominating factors for the determination of their organic vapors adsorption capacity. The GAB isotherm equation fitted the experimental data more closely than the BET equation. The heats of adsorption showed that the adsorption of organic vapors on TNTs was primarily due to physical forces and adsorbates with larger polarity might induce a stronger interaction with TNTs.

Keywords Titanate nanotubes · Adsorption · Organic vapors · Pore structure · Surface chemical characteristics

C.-K. Lee (✉) · S.-S. Liu
Department of Environmental Engineering, Vanung University, Chung-Li 32061, Taiwan
e-mail: anthony@mail.vnu.edu.tw

S.-K. Fen
Department of Civil Engineering, Chung-Yuan Christian University, Chung-Li 32023, Taiwan

H.-P. Chao
Department of Bioenvironmental Engineering, Chung-Yuan Christian University, Chung-Li 32023, Taiwan

F.-C. Huang
Department of Environmental Technology and Management, Taoyuan Innovation Institute of Technology, Chung-Li 32091, Taiwan

1 Introduction

Adsorption-related applications of TNTs derived from hydrothermal method depend on the cation exchange properties, the availability of internal pore volume, and the surface hydrophilicity of TNTs, that are all easily affected by the synthetic conditions, including reaction time, synthesis temperature, acid concentration during washing, and calcination temperature (Kasuga 2006; Lee et al. 2007a, 2007b, 2008a, 2008b; Weng et al. 2006; Yoshida et al. 2005; Yu et al. 2006a, 2006b). With the caion-exchange property and high specific pore volume, TNTs may offer a special environment for adsorption of cations, such as basic dyes and heavy metal ions, through the cation exchange mechanism (Lee et al. 2007a, 2007b, 2008a; Liu et al. 2009; Nie and Teh 2010; Xiong et al. 2010; Sheng et al. 2011; Huang et al. 2012). Moreover, when the sodium cations in TNTs are replaced with other organic cations (such as surfactants) from solution onto TNTs, the surface properties of

Table 1 Properties of selected organic adsorbates (Agnihotri et al. 2005)

Characteristic	Hexane	Cyclohexane	Toluene	MEK
Class	Alkane	Cyclic	Aromatic	Ketone
Molecular formula	C_6H_{14}	C_6H_{12}	C_7H_8	C_4H_8O
Molecular weight (g/mol)	86.18	84.16	92.15	72.11
Heat of vaporization (kJ/mol)	31.9	37.7	39.2	34.1
Dipole moment ($\times 10^{-29}$ C m)	0	0.1	0.13	1.1
Molecular diameter (nm)	0.265	0.429	0.476	0.275
Molecular length (nm)	0.681	0.429	0.568	0.484

TNTs (and then their adsorption ability and capacity) are altered. For instance, when larger organic cations are used, such as hexadecyltrimethylammonium (HDTMA) chloride, the hydrophobic tails interacting with each other may produce an organic phase which acts as a partition medium into which non-ionic organic molecules partition from water. On the other hand, the hydrophobic bonding by conglomeration of large C_{16} alkyl groups associated with HDTMA can render a positive charge development on the surface of TNTs, from which the organic anions (such as acid dyes) can be removed from aqueous solution with anion exchange mechanism (Juang et al. 2008). Volatile organic compounds (VOC), including *n*-hexane, benzene, toluene, *p*-xylene, *m*-xylene, and *o*-xylene, adsorption study of TNTs is fairly recent (Lee et al. 2010). It is found that the adsorption capacity of TNTs positively correlated with their specific surface area and pore volume, and TNTs may be an effective adsorbent for the removal of VOC from gas phase. On the other hand, adsorption capacity for VOC is closely related to adsorbates molecular configuration. Benzene possesses the most effective packing in TNTs and hence the highest adsorption capacity among the examined VOC due to its plate configuration and small molecular size. However, the hydrophilicity of TNTs and the polarity of adsorbates may also play the key factors on the determination of organic vapors adsorption capacity of TNTs. Since the surface of TNTs is rich in hydroxyl groups (Yu and Yu 2006), experimental studies involving select organic molecules with different polarity and well characterized TNTs with different hydrophilicity will contribute to the current state of knowledge about adsorption mechanisms of organic vapors on TNTs.

In this study, we gravimetrically measure the equilibrium adsorption isotherms of *n*-hexane, cyclohexane, toluene, and MEK vapors on hydrothermal derived TNTs characterized with different sodium content. The organic adsorbates are carefully chosen to have similar heats of vaporization (i.e. comparable heats of adsorption) but varying dipole moments and structures (Table 1). The relationship between the alteration in both the pore structures and hydrophilicity of TNTs induced by variation of their sodium contents and the change in the organic vapors adsorption capacity of TNTs is discussed. The experimental data are fitted by the well-known vapor-phase multilayer equations and the isosteric heats of adsorption are calculated, in order to examine the adsorption mechanisms of organic vapors from gas phase onto TNTs.

2 Materials and methods

2.1 Preparation and characterization of TNTs

TNTs (Fig. 1) were prepared via a hydrothermal treatment of TiO_2 powders in a 10 M NaOH solution at 150 °C for 24 h, and subsequently washed with HCl aqueous solution of different concentrations (Kasuga et al. 1998, 1999). The detail processes were given elsewhere (Lee et al. 2008b). It was expected that acid treatment would play an important role in controlling the amount of sodium ions remaining in the TNTs. The amount of residual sodium ions was measured using atomic absorption spectrometry (Z-5000, Hitachi) and was listed in Table 2. For convenience, we denoted the TNTs treated with acid concentrations of 0.1, 0.01, 0.001, 0.0001, and 0.00001 N as S-1 to S-5, respectively (see Table 2). The acid-washed TNTs were dried in a vacuum oven at 110 °C for 8 h and stored in glass bottles for future use.

Effects of acid washing treatment on the microstructures of TNTs were characterized using the transmission electron microscope (TEM), X-ray diffraction (XRD), and nitrogen adsorption-desorption isotherms and were reported in our previous investigations (Lee et al. 2007a, 2008b). According to the TEM images of TNTs (Fig. 1), it can be experimentally concluded that when the sodium content was greater than 1.62 wt.% (or the acid washing concentration is smaller than 0.01 N), the nanotubular structure could be well-preserved and the morphological characteristics of TNTs samples were rather similar. On the other hand, according to the XRD profiles, for S-3 to S-5, a characteristic peak was observed at approximately $2\theta = 10°$, which was considered to correspond to $H_2Ti_3O_7$ or

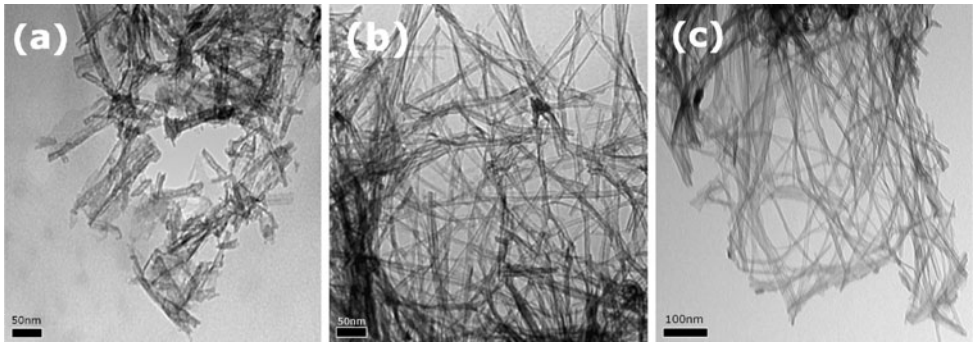

Fig. 1 TEM images of TNTs prepared via a hydrothermal treatment of TiO_2 powders in a 10 M NaOH solution at 150 °C for 24 h, and subsequently washed with (**a**) 0.1 (S-1), (**b**) 0.01 (S-2), and (**c**) 0.00001 N (S-5) HCl aqueous solution

Table 2 Specific surface area, specific pore volume, average pore diameter, and SHI values for the examined TNTs

TNTs sample	Na content (wt.%)	BET surface area (m^2/g)	Total pore volume (cm^3/g)	Pore diameter (nm)	SHI (%)
S-1	0.10	335	1.72	16.4	43
S-2	1.62	373	1.75	14.7	55
S-3	5.93	261	1.14	13.7	14
S-4	6.07	255	1.10	14.1	−31
S-5	6.11	265	1.27	15.5	−5

$Na_xH_{2-x}Ti_3O_7$ crystals. Moreover, for S-2, the peak at approximately $2\theta = 10°$ became diffuse and for S-1, this characteristic peak did not exist. From both the TEM image and XRD pattern of S-1, it can be concluded that when the sodium content of TNTs was approximately 0 wt.% (meaning a nearly complete proton exchange), the aspect ratio (that is, length-to-diameter ratio) was considerably reduced relative to that of other samples. The porous structure characteristics, including BET surface area, pore volume, and pore size, obtained from the conventional analysis of the nitrogen adsorption-desorption isotherms were listed in Table 2. As can be seen from Table 2, both the surface area and pore volume of the examined TNTs were with the decreasing order: S-2 > S-1 > S-5 > S-3 > S-4. These results indicated that if the sodium ions in TNTs were not completely replaced with protons, the lower the sodium content of the TNTs, the higher the specific surface area and pore volume were. The smaller surface area and pore volume of S-1 might be ascribed to its weak nanotubular structure, as shown in Fig. 1, or to the destruction of the layered titanate structure, as shown in the disappearance of the characteristic peak at approximately $2\theta = 10°$ in the XRD patterns.

Effects of acid washing treatment on the hydrophilicity of TNTs were characterized with both FTIR spectra and water vapor isotherms. FTIR spectra were recorded using a Perkin Elemer Model 1600 FTIR spectrophotometer over the range of 4000–400 cm^{-1} with a scan rate of 0.2 cm/s. IR spectra were obtained in the KBr disks. Water adsorption isotherms of the TNTs were obtained at 15 °C in the range of relative pressure to 0.82 (Cahn D-200 microbalance). Surface hydrophobicity of the TNTs was evaluated numerically by using the surface hydrophobicity index (SHI) defined as follows (Ooka et al. 2004):

$$\text{SHI}\ (\%) = \left(1 - \frac{\text{BET surface area in water adsorption}}{\text{BET surface area in nitrogen adsorption}}\right) \times 100\ \%. \quad (1)$$

It should be noted that larger SHI values would imply higher surface hydrophobicity.

2.2 Adsorption of organic vapors

The isotherms of *n*-hexane, cyclohexane, toluene, and MEK were measured with a Cahn D-200 microbalance in a constant volume system. *ca.* 100 mg of the adsorbents were used. All adsorbates used were GR grade from Merck Co. Equilibrium was assumed when the sample weight changed by less than 0.01 mg in 1 h. A complete adsorption isotherm was constructed by increasing the pressure in a step-wise manner. The temperature of the system was controlled to within ±1 °C by recirculating refrigerant from a thermal stat. The pressure of the system was measured using two MKS Baratron type 122A absolute pressure transducers within 0–10 and 1–1000 torr ranges. These pressure transducers had four digits of resolution. The effect of temperature on the adsorption data was studied by performing the adsorption experiments at various temperatures (20 and 25 °C).

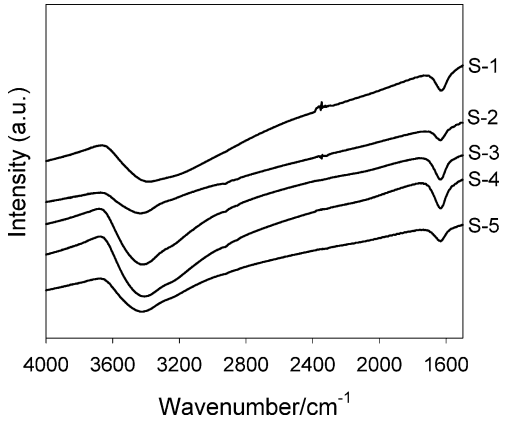

Fig. 2 FTIR spectra of the examined TNTs

3 Results and discussion

3.1 Effects of acid washing treatment on the hydrophilicity of TNTs

Infrared spectra shown in Fig. 2 indicates that there is a large amount of water and hydroxyl groups existed in the TNTs because of the existence of a bending vibration of H-O-H at 1630 cm^{-1} and a strong stretching vibration of O-H at 3400 cm^{-1} (Yu and Yu 2006). Moreover, it is found that the strength of the absorbance near 3400 cm^{-1} increases with the increase of sodium content in the TNTs. This result indicates that the increase of sodium content may induce an increase in the surface hydrophilicity of TNTs, which can be further verified with the variation of SHI values.

Adsorption isotherms of water and nitrogen vapor on the TNTs are shown in Fig. 3. From the comparison between the isotherms of water and those of nitrogen in Fig. 3, the difference among the TNTs in water adsorption isotherms is larger than that in nitrogen adsorption ones. This indicates that there is large difference in the surface hydrophobicity from TNTs to TNTs. The hydrophobicity of TNTs is evaluated and compared by using SHI value. As shown in Table 2, the SHI value of TNTs varies in the range from −31 to 55 % and increases in the order S-4 < S-5 < S-3 < S-1 < S-2, which is consistent with the result of FTIR spectra. As listed in Table 2, since the increase in the Na-content may induce an obvious variation in both surface area (and pore volume) and hydrophobicity of TNTs, the selected TNTs may be good candidates for the examination of the effects of pore structure and surface chemical characteristics on the determination of adsorption capacity of organic vapors with different polarity and molecular configuration.

3.2 Adsorption isotherms

Equilibrium isotherms of *n*-hexane, cyclohexane, toluene, and MEK, on S-1 to S-5 samples at 25 °C are demonstrated in Fig. 4. All adsorption isotherms are typically of IUPAC Type II in shape, characterizing the formation of multiple layers of adsorbate molecules on the TNTs surface and a large uptake being observed when the saturation pressure is nearly reached. Moreover, the trend of organic vapors adsorption capacities on TNTs is closely related to the adsorbates properties. For all examined organic vapors, S-2 possesses the largest adsorption capacity, because it has the highest specific surface area and pore volume among the examined TNTs samples although it has weak hydrophilicity. On the other hand, S-3 possesses the lowest adsorption capacity because it has low specific surface area and pore volume, and intermediate hydrophilicity among the examined TNTs.

For the adsorption of vapors on nanotubes, the adsorption behavior may be a combination of adsorption [i] in the hollow space inside nanotubes, [ii] in the interstitial spacing between three or more neighboring nanotubes, [iii] on the furrows present on the periphery of a nanotube bundle, and [iv] on the curved surface on the periphery of a bundle (Agnihotri et al. 2004). In such a case, it would mean that at low relative pressure, adsorption would mainly occur on sites [i], [ii], and [iii], and at higher relative pressure, organic vapor adsorption occurs entirely on the external surface of the bundles (i.e., site [iv]). Since the adsorption capacity on sites [i], [ii], and [iii] is closely related their specific surface area and pore volume, and the multilayer adsorption on site [iv] may be directly proportional to the external surface area of the TNTs bundles, both the specific surface area and pore volume of TNTs samples may be the dominating factors on the determination of their adsorption capacity for organic vapors. However, if the surface area and pore volume of TNTs are not large enough and the polarity of organic vapors is strong, the surface hydrophilicity of TNTs may also play a key factor on the determination of the adsorption capacity of organic vapors in addition to both specific surface area and pore volume.

It is interesting to note that the adsorption capacity of S-1 sample differs considerably for different organic vapors. For adsorbates with lower polarity (*n*-hexane and cyclohexane), S-1 still has high adsorption capacity, while for adsorbates with higher polarity (toluene and MEK), it has the low adsorption capacity when compared to other TNTs samples. The specific surface area and pore volume are high in case to S-1, but its surface hydrophilicity is weak among the examined TNTs. The low adsorption capacity of high polarity adsorbates on S-1 indicates that the surface hydrophilicity, but not specific surface area and pore volume, plays a key factor on the determination of adsorption capacity. On the contrast, although the specific surface area and pore volume of S-4 and S-5 are low, they still possess high adsorption capacity for high polarity adsorbates (toluene and MEK) due to their stronger hydrophilicity when compared to other TNTs samples.

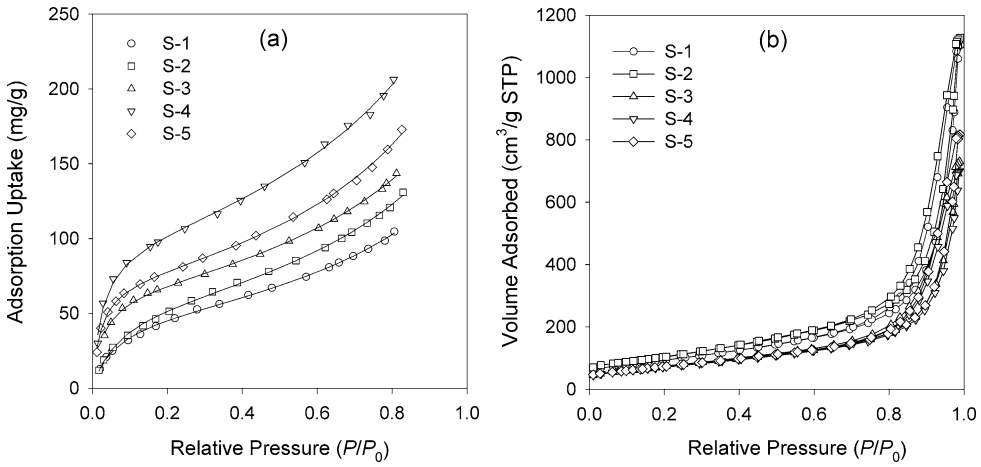

Fig. 3 Adsorption isotherms of (**a**) water vapor at 15 °C and (**b**) nitrogen on the examined TNTs

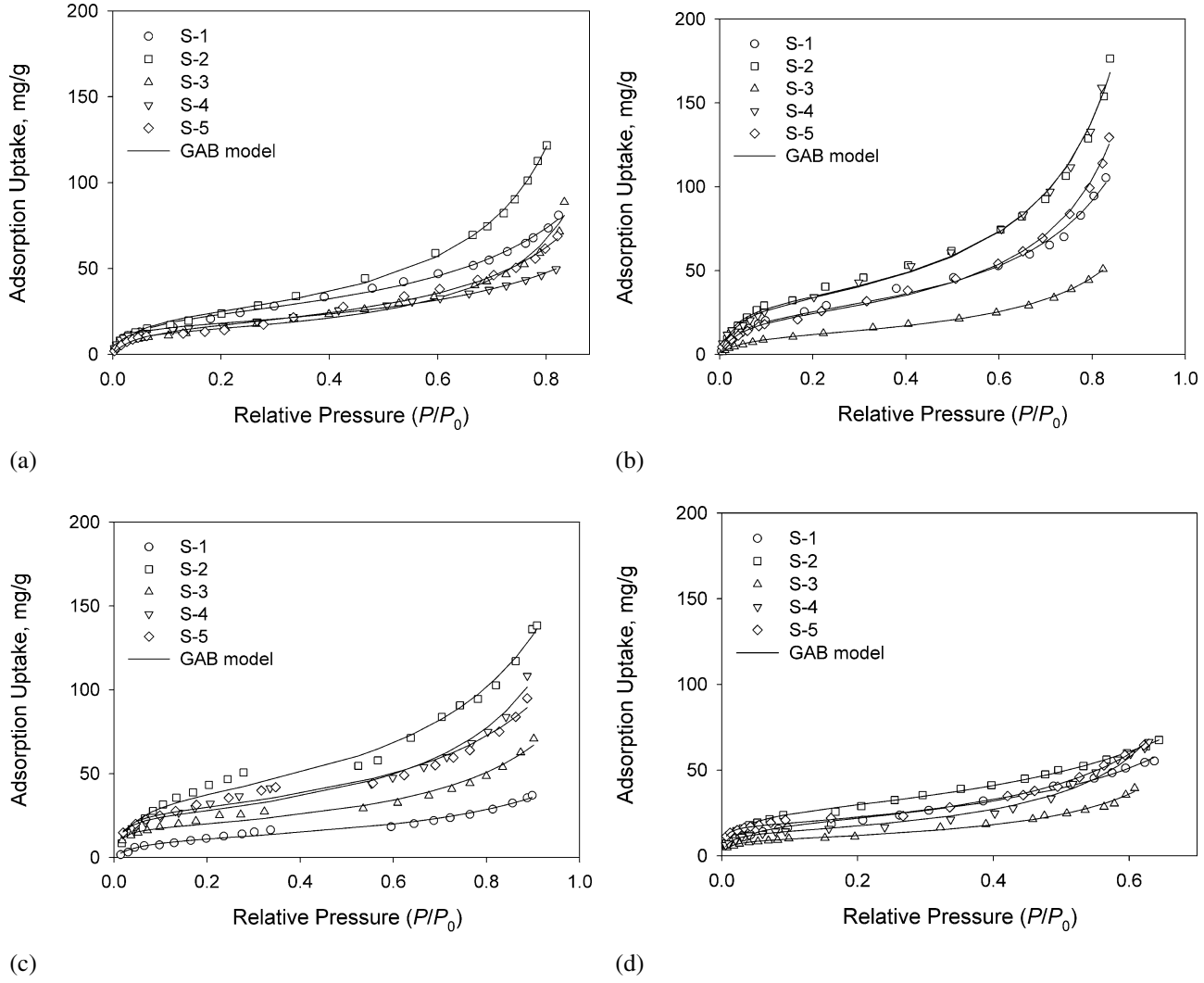

Fig. 4 Adsorption isotherms of organic vapors on the examined TNTs at 25 °C; (**a**) *n*-hexane, (**b**) cyclohexane, (**c**) toluene, and (**d**) MEK

Figure 5 compares the adsorption capacities of four examined organic vapors on the S-2 sample. The general trend of organic vapors adsorption capacities on S-2 is with the decreasing order MEK > cyclohexane > toluene > *n*-hexane. Since the S-2 has high specific surface area and pore volume and weak hydrophilicity, the difference in the adsorp-

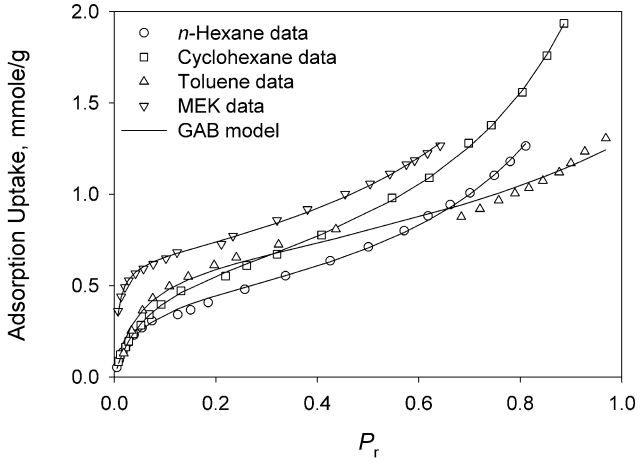

Fig. 5 Adsorption isotherms of organic vapors on S-2 sample at 20 °C

tion capacity for the examined adsorbates may be mainly ascribed to the molecular configuration difference existing on the examined organic vapors (Chiang et al. 1991). As shown in Table 1 and Fig. 5, the adsorption capacities are inverse proportional to the molecular length of adsorbates. Since its small molecular diameter and length, MEK possesses the most effective packing in the S-2 and then the highest adsorption capacity among the examined organic vapors. On the other hand, the low adsorption capacity of *n*-hexane may be due to the ineffective packing in S-2 induced by its linear configuration. For cyclohexane and toluene, the adsorption capacity of toluene is smaller than that of cyclohexane, because toluene possesses larger molecular diameter and length.

3.3 Isotherm modeling

The experimental data are fitted to BET (Brunauer et al. 1938; Hill 1960) and GAB (Anderson 1946; De Boer 1953; Clark 1970) multilayer isotherm models for future simulation. The equation for the BET model is

$$\frac{P_r}{(1-P_r)W} = \frac{1}{W_m C} + \frac{P_r(C-1)}{W_m C}, \tag{2}$$

where P_r is the relative pressure, W the equilibrium uptake, W_m the monolayer capacity, and C a constant related to the net heat of adsorption as follows

$$C = C_0 \exp\left[(q_L - q_1)/RT\right], \tag{3}$$

where $C_0 \approx 1.0$, q_1 is the heat of adsorption in the first layer, and q_L is the heat of liquefaction. Equation (2) can also be derived based on kinetic considerations or by using statistical thermodynamics (Hill 1960).

Since the BET model is based on a number of rather serious idealizations and has some limitations on practical applications, many modified versions of BET model were proposed. Among them, Anderson, De Boer, and Guggenheim (Anderson 1946; De Boer 1953; Clark 1970) improved the BET theory by assuming that the heat of adsorption of the second to approximately ninth layers differed from the heat of liquefaction by a constant amount, and that the heat of adsorption was equal to the heat of liquefaction in the layers following these. The final GAB model equation has the following form

$$\frac{W}{W_m} = \frac{CkP_r}{(1-kP_r)(1-kP_r+CkP_r)}, \tag{4}$$

where W, W_m, and C are the same as defined in the BET equation, and the additional k represents the difference between the heat of adsorption of the multilayers and the heat of liquefaction. Thus, k is a measure of the attractive force field strength and can be expressed as

$$k = k_0 \exp\left[(q_2 - q_L)/RT\right]. \tag{5}$$

The results of the data fitted to the BET and GAB models, including the average percentage deviations of the predicted isotherms from the experimental ones, are presented in Table 3. The predicted values are shown as lines in Fig. 4. The best fit model parameters are obtained by using a nonlinear regression analysis. The standard deviation (SD) is calculated from the following expression

$$\mathrm{SD}\ (\%) = 100\sqrt{\frac{\sum[(W^{cal} - W^{exp})/W^{exp}]^2}{n-1}} \tag{6}$$

where n is the number of data points, and the superscripts "cal" and "exp" refer to the calculated and measured adsorption capacity, respectively (Lin and Juang 2002).

As shown in Table 3, the GAB model provides much better overall predictions than does the BET model. For GAB model, the SD for the entire relative pressure range is in a range varying from 1.76 to 11.37 %. In general, the BET model can predict the experimental data accurately for a relative pressure less than 0.4 (monolayer region). In the multilayer region, however, the SD is greatly increased and for some cases (such as toluene), the fitness of the BET model to the experimental data is difficult to estimate. This could be attributed to the oversimplifying assumptions of the BET model concerning the multilayer region. Model parameters for both BET and GAB equations show no definite trend with increasing temperature (Lee et al. 2010; Dural and Chen 1997).

3.4 Isosteric heat of adsorption

Adsorption isotherms of organic vapors on S-2 at 20 and 25 °C are demonstrated in Fig. 6. Vapor-phase adsorption of organic vapors by the TNTs is an exothermic process, as indicated by a downward shift of the isotherms with increasing temperature. This is in agreement with the

Table 3 Model analysis for organic vapors adsorption on TNTs

TNTs sample	T (°C)	BET			GAB			
		W_m	C	SD (%)	W_m	C	k	SD (%)
n-Hexane								
S-1	25	15.91	75.56	13.80	22.32	29.65	0.88	10.38
S-2	20	24.87	85.78	24.92	37.89	28.04	0.82	5.10
	25	24.04	22.05	12.80	22.95	25.84	1.01	10.49
S-3	25	13.43	41.22	8.62	13.11	44.94	1.01	8.14
S-4	25	10.90	267.30	18.92	16.15	75.71	0.83	7.86
S-5	25	13.09	50.74	11.06	16.29	24.26	0.93	8.22
Cyclohexane								
S-1	25	19.12	48.62	24.69	24.18	26.50	0.92	8.12
S-2	20	23.94	146.53	35.95	48.57	21.50	0.80	5.50
	25	28.22	46.64	15.39	31.07	34.95	0.97	9.57
S-3	25	9.55	37.19	12.79	11.41	22.58	0.94	3.85
S-4	25	28.58	38.48	10.64	31.02	29.41	0.98	8.83
S-5	25	21.15	32.16	12.87	22.80	24.80	0.98	10.14
Toluene								
S-1	25	–	–	–	11.23	26.82	0.77	11.28
S-2	20	–	–	–	58.43	42.63	0.52	11.25
	25	–	–	–	36.16	33.31	0.81	11.37
S-3	25	–	–	–	17.54	117.31	0.82	8.71
S-4	25	–	–	–	24.43	90.73	0.86	8.81
S-5	25	–	–	–	26.79	85.27	0.79	7.42
MEK								
S-1	25	20.75	28.92	13.40	19.16	36.31	1.05	10.08
S-2	20	37.08	579.08	10.25	46.27	192.99	0.78	1.76
	25	24.83	57.43	5.07	25.98	51.53	0.96	3.89
S-3	25	13.43	23.25	19.48	9.22	90.45	1.24	5.10
S-4	25	23.32	9.66	36.93	13.43	89.25	1.28	6.62
S-5	25	21.93	85.82	11.84	17.45	231.66	1.18	3.80

fact that the physical adsorption forces, such as Van der Waal's force, are expected to be weaker at higher temperatures.

The heat of adsorption provides a direct measure of the strength of the binding forces between the adsorbate and adsorbent. Quantification of adsorption heat is important for adsorption kinetic studies because the heat released upon adsorption is partly absorbed by the adsorbent, which raises the adsorbent's temperature and thus slows the rate of adsorption as equilibrium is approached. The isosteric heats of adsorption, q_{st}, can be calculated from the adsorption data obtained at multiple temperatures (Fig. 6) using the Clasius-Clapeyron equation (Young and Crowell 1962)

$$q_{st} = R\left[\partial \ln P/\partial(1/T)\right]_W \quad (7)$$

where R is gas constant, P the equilibrium gas pressure, T the temperature, and W the amount of vapor adsorption. As shown in Fig. 7, the heats of adsorption are 1–4 times the heats of vaporization for each respective organic vapor (the heat of vaporization for the examined organic vapors is about 30−40 kJ/mol), which confirms that the adsorption of organic vapors on S-2 is basically physical adsorption. The dependence of the heat of adsorption on loading is an indication that adsorption is occurring on different types of sites, i.e., S-2 has an energetically heterogeneous surface. Moreover, the general trend of heat of adsorption is similar

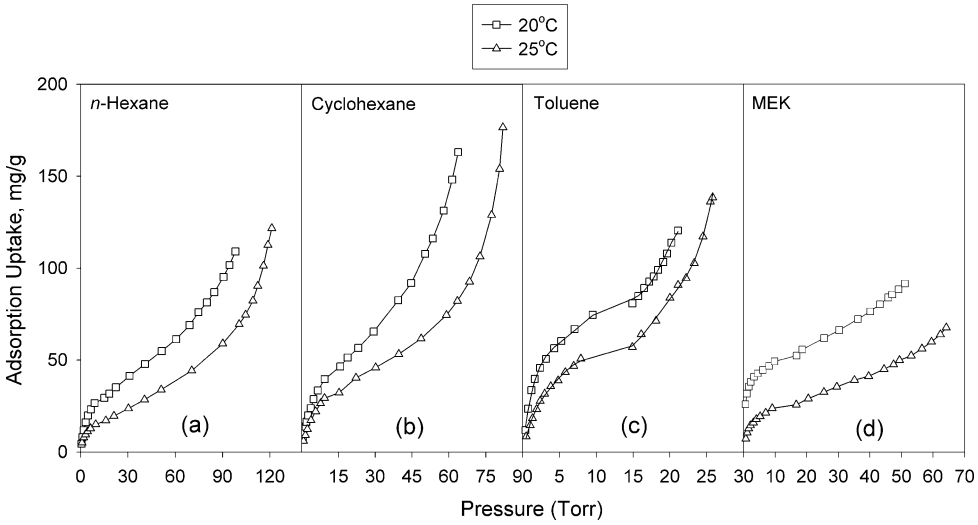

Fig. 6 Adsorption isotherms of organic vapors on S-2 sample at 20 and 25 °C; (**a**) *n*-hexane, (**b**) cyclohexane, (**c**) toluene, and (**d**) MEK

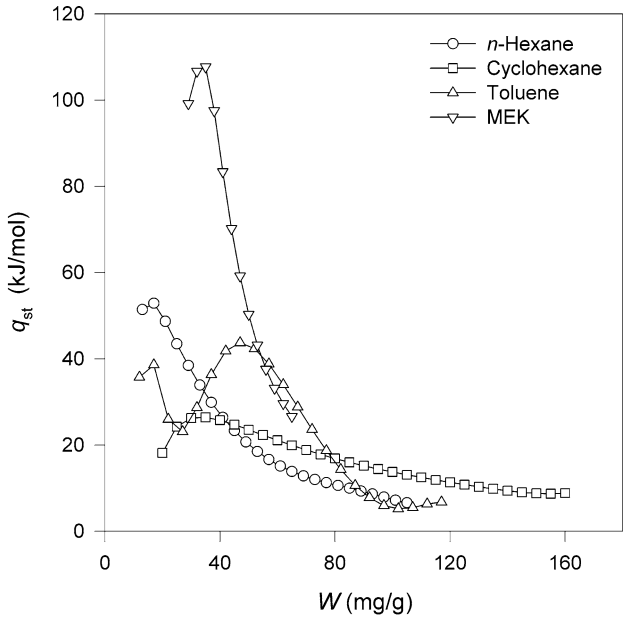

Fig. 7 Variation of isosteric heat of adsorption with increasing organic vapors adsorption on S-2 sample

to the trend for the dipole moments of organic vapors (see Table 1). Significantly higher heat of adsorption for MEK, which has the highest dipole moment of 1.1×10^{-29} C m of the organic vapors tested here, suggests although S-2 sample has weak hydrophilicity among the examined adsorbents, it still has a polar surface.

It should be noted that the heat curve of toluene displays a complex variation with the coverage, which is not in consistent with the general trend for the heat curve of a multilayer adsorption. The feature in the heat curves is that a maximum of unusual height is found at high loadings, and even it has a q_{st} higher than that in monolayer region. From this result, it seems to imply that the interaction between the toluene molecules is stronger than that between the toluene molecule and unoccupied sorption sites.

4 Conclusions

Gravimetric methods were used to determine the equilibrium adsorption capacities of *n*-hexane, cyclohexane, toluene, and MEK on hydrothermal derived TNTs at isothermal conditions of 20 and 25 °C. It was found that the increase in the Na-content (or the decrease in the acid washing concentration) might induce a decrease in both surface area (and pore volume) and hydrophobicity of TNTs. The isotherms of organic vapors on all examined TNTs were type II and sigmoidal in shape. If the specific surface area and pore volume of TNTs were enough large to overcome the impacts of polarity of both adsorbent and adsorbate on the adsorption capacity, they might possess high adsorption capacity, as shown in the S-2 sample. On the other hand, adsorption capacity for organic vapors was closely related to their molecular configuration. MEK possessed the most effective packing in TNTs and hence the highest adsorption capacity among the examined organic vapors due to its small molecular diameter and length. The GAB isotherm equation fitted the experimental data more closely than the BET equation. The heat of adsorption of organic vapors on S-2 sample was 1–4 times its heat of vaporization, which was typical for physical adsorption. The shape of the heat curves was an indication that the TNTs sample was characterized by energetically heterogeneous surfaces. Furthermore, the general trend of heat of adsorption was similar to the trend for the dipole moments of the organic vapors, suggested that although S-2 has weak hydrophilicity among the examined TNTs, it still has a polar surface.

Acknowledgements This work was supported by the grant NSC99-2221-E-238-010 of National Science Council (Taiwan, ROC).

References

Agnihotri, S., Rostam-Abadi, M., Rood, M.J.: Temporal changes in nitrogen adsorption properties of single-walled carbon nanotubes. Carbon **42**, 2699–2710 (2004)

Agnihotri, S., Rood, M.J., Rostam-Abadi, M.: Adsorption equilibrium of organic vapors on single-walled carbon nanotubes. Carbon **43**, 2379–2388 (2005)

Anderson, R.B.: Modifications of the Brunauer, Emmett and Teller equation. J. Am. Chem. Soc. **68**, 686–691 (1946)

Brunauer, S., Emmett, P.H., Teller, E.: Adsorption of gases in multimolecular layers. J. Am. Chem. Soc. **60**, 309–319 (1938)

Chiang, A.S.T., Lee, C.K., Chang, Z.H.: Adsorption and diffusion of aromatics in $AlPO_4$-5. Zeolites **11**, 380–386 (1991)

Clark, A.: The Theory of Adsorption. Academic Press, New York (1970)

De Boer, J.H.: The Dynamical Character of Adsorption. Clarendon, Oxford (1953)

Dural, N.H., Chen, C.H.: Analysis of vapor phase adsorption equilibrium of 1,1,1-trichloroethane on dry soils. J. Hazard. Mater. **53**, 75–92 (1997)

Hill, T.L.: Statistical Mechanics. McGraw-Hill, New York (1960)

Huang, J., Cao, Y., Liu, Z., Deng, Z., Tang, F., Wang, W.: Efficient removal of heavy metal ions from water system by titanate nanoflowers. Chem. Eng. J. **180**, 75–80 (2012)

Juang, L.C., Lee, C.K., Wang, C.C., Hung, S.H., Lyu, M.D.: Adsorptive removal of acid red 1 from aqueous solution with surfactant modified titanate nanotubes. Environ. Eng. Sci. **25**(4), 519–528 (2008)

Kasuga, T.: Formation of titanium oxide nanotubes using chemical treatments and their characteristic properties. Thin Solid Films **496**, 141–145 (2006)

Kasuga, T., Hiramatsu, M., Hoson, A., Sekino, T., Niihara, K.: Formation of titanium oxide nanotube. Langmuir **14**, 3160–3163 (1998)

Kasuga, T., Hiramatsu, M., Hoson, A., Sekino, T., Niihara, K.: Titania nanotubes prepared by chemical processing. Adv. Mater. **11**, 1307–1311 (1999)

Lee, C.K., Liu, S.S., Juang, L.C., Wang, C.C., Lyu, M.D., Hung, S.H.: Application of titanate nanotubes for dyes adsorptive removal from aqueous solution. J. Hazard. Mater. **148**, 756–760 (2007a)

Lee, C.K., Wang, C.C., Lyu, M.D., Juang, L.C., Liu, S.S., Hung, S.H.: Effects of sodium content and calcination temperature on the morphology, structure, and photocatalytic activity of nanotubular titanates. J. Colloid Interface Sci. **316**, 347–354 (2007b)

Lee, C.K., Lin, K.S., Wu, C.F., Lyu, M.D., Lo, C.C.: Effects of synthesis temperature on the microstructures and basic dyes adsorption of titanate nanotubes. J. Hazard. Mater. **150**, 494–503 (2008a)

Lee, C.K., Wang, C.C., Juang, L.C., Lyu, M.D., Hung, S.H., Liu, S.S.: Effects of sodium content on the microstructures and basic dye cation exchange of titanate nanotubes. Colloids Surf. A, Physicochem. Eng. Asp. **317**, 164–173 (2008b)

Lee, C.K., Chen, H.C., Liu, S.S., Huang, F.C.: Effects of acid washing treatment on the adsorption equilibrium of volatile organic compounds on titanate nanotubes. J. Taiwan Inst. Chem. Eng. **41**(3), 373–380 (2010)

Lin, S.H., Juang, R.S.: Heavy metal removal from water by sorption using surfactant-modified montmorillonite. J. Hazard. Mater. **92**, 315–326 (2002)

Liu, S.S., Lee, C.K., Chen, H.C., Wang, C.C., Juang, L.C.: Application of titanate nanotubes for Cu(II) ions adsorptive removal from aqueous solution. Chem. Eng. J. **147**(2–3), 188–193 (2009)

Nie, X.T., Teh, Y.L.: Titanate nanotubes as superior adsorbents for removal of lead(II) ions from water. Mater. Chem. Phys. **123**, 494–497 (2010)

Ooka, C., Yoshida, H., Suzuki, K., Hattori, T.: Highly hydrophobic TiO_2 pillared clay for photocatalytic degradation of organic compounds in water. Microporous Mesoporous Mater. **67**, 143–150 (2004)

Sheng, G., Yang, S., Sheng, J., Zhao, D., Wang, X.: Influence of solution chemistry on the removal of Ni(II) from aqueous solution to titanate nanotubes. Chem. Eng. J. **168**, 178–182 (2011)

Weng, L.Q., Song, S.H., Hodgson, S., Baker, A., Yu, J.: Synthesis and characterisation of nanotubular titanates and titania. J. Eur. Ceram. Soc. **26**, 1405–1409 (2006)

Xiong, L., Yang, Y., Mai, J., Sun, W., Zhang, C., Wei, D., Chen, Q., Ni, J.: Adsorption behavior of methylene blue onto titanate nanotubes. Chem. Eng. J. **156**, 313–320 (2010)

Yoshida, R., Suzuki, Y., Yoshikawa, S.: Effects of synthetic conditions and heat-treatment on the structure of partially ion-exchanged titanate nanotubes. Mater. Chem. Phys. **91**, 409–416 (2005)

Young, D.M., Crowell, A.D.: Physical Adsorption of Gases. Butterworth, London (1962)

Yu, J., Yu, H.: Facile synthesis and characterization of novel nanocomposites of titanate nanotubes and rutile nanocrystals. Mater. Chem. Phys. **100**, 507–512 (2006)

Yu, J., Yu, H., Cheng, B., Trapalis, C.: Effects of calcination temperature on the microstructures and photocatalytic activity of titanate nanotubes. J. Mol. Catal. A, Chem. **249**, 135–142 (2006a)

Yu, H., Yu, J., Cheng, B., Zhou, M.: Effects of hydrothermal post-treatment on microstructures and morphology of titanate nanoribbons. J. Solid State Chem. **179**, 349–354 (2006b)